Proceedings of the
Annual Stability Conference
Structural Stability Research Council
Atlanta, Georgia, April 21-24, 2020

Simplified solutions for estimating the lateral-torsional buckling resistance of nonprismatic girders

Matthew C. Reichenbach[1], Todd A. Helwig[2], Michael D. Engelhardt[3]

Abstract
Lateral-torsional buckling is a complex limit state that is often complicated by the presence of singly-symmetric and/or nonprismatic sections, which are common in composite construction. Estimating the buckling resistance of nonprismatic beams under uniform moment or moment gradients can be challenging. There are no general hand solutions readily available, and procedures for evaluating the buckling behavior of these relatively common cases are either absent from specifications or are overly simplified and have not been validated. This paper focuses on the development of a simplified weighted-average approach for approximating the buckling resistance of singly-symmetric and nonprismatic beams under uniform moment. A detailed parametric study including a wide range of parameters such as various intermediate bracing schemes and stepped flange transitions was conducted. The proposed design methodology was evaluated based on its ability to approximate the finite element solutions.

1. Introduction
Lateral-torsional buckling (LTB), a limit state that often governs the design of steel I-girders in buildings and bridges, must be evaluated for all stages of construction and throughout the service life of a structure. With built-up I-sections often being singly-symmetric and nonprismatic, predicting the buckling behavior can be challenging.

Most steel girders are designed to act compositely with the concrete slab, which typically results in a top flange smaller in size than the corresponding bottom flange and a cross-section with a single plane of symmetry. The buckling behavior of singly-symmetric sections are often more complex than the buckling behavior of doubly-symmetric shapes.

To further complicate the LTB behavior, engineers often transition flanges and webs at discrete locations along the length of the span to accommodate variations in stress and to improve efficiency in moderate- to long-span girders. Transitions in built-up, nonprismatic beams generally include some combination of a change in plate thickness and/or width of flanges and webs.

[1] Graduate Research Assistant, The University of Texas at Austin, <reichenbach.matt@utexas.edu>
[2] Professor, The University of Texas at Austin, <thelwig@ mail.utexas.edu >
[3] Professor, The University of Texas at Austin, <mde@mail.utexas.edu>

Although web-tapered members are sometimes used in building and bridge applications, the focus of this study was sections with constant depth webs and stepped flanges.

LTB is especially critical during construction when bracing of noncomposite beams may be limited and/or the concrete slab has not cured. Since bracing conditions can vary substantially during erection and construction, long unbraced lengths with multiple flange transitions are frequently encountered. In the finished composite structure, there is also uncertainty regarding the negative moment region of continuous girders, where the bottom flange is discretely braced at cross-frame or diaphragm locations.

While nonprismatic sections are common in practice, most specifications provide little to no guidance on the evaluation of the LTB capacity of these sections. This paper focuses on the development of a simplified design approach for evaluating the LTB behavior of singly-symmetric girders under uniform-moment loading, considering both prismatic and nonprismatic sections. The study includes a wide range of parameters such as the degree of monosymmetry and the location of flange transitions. For the effects of moment gradient on the LTB responses of these beams, refer to Reichenbach et al. (2019).

Following the introductory section, pertinent background information is outlined, and an overview of the modeling decisions and range of parameters considered in the finite element analysis (FEA) study is provided. Proposed design solutions are then presented, and finite element results are subsequently compared to the simplified design procedures.

2. Background

Given the complexities of the lateral-torsional buckling limit state, most design specifications have adopted simplified, approximate approaches for estimating the resistance of a beam. These simplified approaches make use of solutions derived for uniform-moment loading and employ approximate correction factors (C_b) to account for the benefits of moment gradient. The focus of the present study is on the expressions for uniform-moment loading, specifically as it pertains to singly-symmetric and/or nonprismatic sections. The following subsections provide a brief overview on the current state of design practice for these complex sections, as well as outline the primary objectives of the study.

2.1 Singly-Symmetric Sections

The uniform-moment solution for LTB that is the most familiar to engineers is the expression developed by Timoshenko (1961), which represents the exact solution for doubly-symmetric, prismatic sections. While this expression for doubly-symmetric shapes is relatively simple to use, expressions for singly-symmetric shapes generally increase in complexity. The exact, elastic LTB solution for singly-symmetric sections under uniform moment is given by the following expressions (Galambos 1968, Ziemian 2010):

$$M_{cr,th} = \frac{\pi^2 E I_y}{{L_b}^2}\left\{\frac{\beta_x}{2} + \sqrt{\left(\frac{\beta_x}{2}\right)^2 + \left[\frac{C_w}{I_y} + \frac{GJ}{EI_y}\frac{{L_b}^2}{\pi^2}\right]}\right\} \tag{1}$$

$$\beta_x = \frac{1}{I_x}\int_A y(x^2 + y^2)dA - 2y_o \tag{2}$$

where E is the modulus of elasticity, I_y is the weak-axis moment of inertia of the section, L_b is the unbraced length of the beam segment, C_w is the warping constant, G is the elastic shear modulus, J is the St. Venant torsional constant, β_x is the coefficient of monosymmetry, I_x is the major-axis moment of inertia, x and y are the centroidal coordinates, and y_o is the distance between the shear center and the centroid. The integration in Eq. 2 is performed over the cross-sectional area, A. The subscript "th" in Eq. 1 is to signify that the solution is theoretical and to differentiate this value from the finite element solutions presented later. Also note that this expression reduces to the Timoshenko expression (1961) for doubly-symmetric shapes.

The expression for the monosymmetry parameter in Eq. 2 is generally not practical for design. Consequently, most design specifications employ approximate LTB solutions for singly-symmetric sections that are generally within 10-15% of the exact solution in Eq. 1. While the simplified solutions could have been used for comparison in this paper, the potential conservatism or unconservatism would likely detract from the measure of accuracy of the proposed approach. Therefore, FEA results herein are compared to the exact, theoretical solution given in Eq. 1 and not the more popular, simplified expressions.

2.2 Nonprismatic Sections

Eq. 1 was derived specifically for doubly-symmetric or singly-symmetric shapes with constant section properties (namely J, C_w, and I_y) along the unbraced length and does not explicitly address nonprismatic sections. In fact, little guidance is generally found for nonprismatic sections under uniform-moment loading. AISC (2016) currently provides no guidance, and the American Association of State Highway and Transportation Officials (AASHTO) LRFD Bridge Design Specifications (2017) employ an overly conservative approach to quantify the LTB resistance of nonprismatic girder segments.

Similarly, previous research has predominantly focused on the LTB behavior of prismatic sections (Helwig et al. 1997). Several researchers have developed methods to quantify the effects of nonprismatic sections (namely stepped flanges) on the LTB behavior of unbraced beam segments; however, those proposed procedures were either not for general-use or were too complex for implementation into design specifications (Trahair 1993, Park 2003, Gelera 2012, Grubb and Schmidt 2012, Slein and White 2019).

2.3 Research Objectives

The lack of guidance provided by current design specifications served as the impetus for the study documented herein, which is summarized by the following question: can the LTB expressions derived for prismatic beams be modified or adjusted to accommodate generic nonprismatic sections using simple approaches and providing results within acceptable levels of accuracy?

Results from a parametric finite element study were used to develop a proposed hand-calculation technique. The accuracy of the proposed methodology is evaluated by comparing the critical buckling moments from the theoretical Eqs. 1 and 2 ($M_{cr,th}$) and the critical buckling moment determined by FEA methods ($M_{cr,FEA}$). The proposed technique is based upon a length-weighted average method, similar to but more general than the work conducted by Trahair (1993). For these approaches, the nonprismatic segment is treated as a prismatic segment of equal unbraced length with effective section properties. Weighted-average approaches have also been previously investigated for stability bracing expressions (Han and Helwig 2017). These simplified methods are easy to interpret and apply in practice, making them attractive solutions for this complex problem.

3. Overview of Parametric Study

The variables considered in the parametric FEA studies included: (i) span-to-depth ratio and intermediate bracing scheme, (ii) degree of monosymmetry, and (iii) variation in flange transitions (degree of nonprismatic variation). With these parameters in mind, a total of 14,040 unique girders (both prismatic and nonprismatic) were evaluated as part of the uniform moment study. As discussed previously, the effects of moment gradient are not addressed in the paper. Instead, refer to Reichenbach et al. (2019) for similar parametric studies on beams subjected to various moment gradients.

The authors believe that the resulting design methodology would undoubtedly increase in complexity if extreme ranges of parameters are considered, which would in turn increase the probability of misinterpretation and errors. The intent of the investigation was not to consider every possible geometry or condition, but rather focus on systems that fall within practical ranges most commonly encountered in design. The following subsections outline the range of parameters evaluated for each of the three primary variables introduced above.

3.1 Span-to-Depth Ratio and Intermediate Bracing

Span-to-web depth ratios of 15, 20, 25, and 30 were considered, which are representative of the conditions commonly found in practice. Within each of the span-to-depth ratios considered, different bracing schemes were also evaluated for their effect on the LTB behavior. Braces only at the ends ($L_b = L$) and intermediate bracing schemes of one-half ($L_b = L/2$) and one-third ($L_b = L/3$) of the span length were considered, which produced unbraced length-to-depth ratios of {7.5, 10, 12.5, 15} and {5, 6.67, 8.33, 10}, respectively. The cases with larger unbraced lengths are representative of steel girders during erection, and cases with smaller brace spacing are representative of girders during deck casting and in the final constructed state.

3.2 Degree of Monosymmetry

The relative size of top and bottom flanges in singly-symmetric sections is often characterized by the degree of monosymmetry, ρ, or the ratio of the weak-axis moment of inertia of the compression flange to the weak-axis moment of inertia of the entire section. The degree of monosymmetry for doubly-symmetric sections, for which the top and bottom flange dimensions are identical, is 0.5 (neglecting the small I_y contributions from the web plate). The parametric study was conducted with ρ-values ranging from 0.1 to 0.9, which is similar to the limits allowed in AASHTO Section 6.10.2.2 ($0.091 \leq \rho \leq 0.91$). Sections that do not satisfy these limits are essentially T-sections, for which the LTB behavior is difficult to predict analytically due to the increased susceptibility to web distortion and local buckling. As such, sections outside of this range were excluded from the study.

Depending on the application of the uniform-moment loading, either the top or bottom flange could be considered the compression flange. As such, the degree of monosymmetry is taken with respect to the top flange in this paper for consistency. Therefore, ρ_{top} is defined as the ratio between the weak-axis moment of inertia of the top flange and the weak-axis moment of inertia of the entire section (neglecting the web plate):

$$\rho_{top} = \frac{I_{y,top}}{I_y} \tag{3}$$

For practical composite girder applications, sections in positive moment regions (top flange in compression) often possess ρ_{top} ratios between 0.2 to 0.5, for which the size of the top flange is smaller than or equal to the size of the bottom flange. In contrast, sections in negative moment regions (bottom flange in compression) are often doubly-symmetric ($\rho_{top} = 0.5$) or close to doubly-symmetric. In any case, beams with ρ_{top} values greater than 0.5 are relatively uncommon. Although results for ρ_{top} outside of the practical range are presented in this paper for completeness, the primary focus is intended for sections that occur the most often in practice where $0.2 \leq \rho_{top} \leq 0.5$.

Additionally for nonprismatic beams, the ρ_{top} ratio may not be uniform along the unbraced length. Thus, the ρ_{top} values reported in the subsequent results correspond to the monosymmetry of the smallest cross-section, or the base section, which is identified as $\rho_{top,base}$. The flange sizes in unique cross-sections other than the base section are indicated as multipliers applied to the base section, as discussed in the next subsection.

Section proportions were selected to narrow the focus solely on the LTB behavior and not local buckling effects. Thus, the distance between the flange centroids was fixed at 60 inches, and the web thickness was fixed at 7/8 inches. The effective web slenderness ($2D_c/t_w$ where D_c is the web depth in compression and t_w is the web thickness) satisfied the compact web slenderness limits for grade 50 steel as a means to preclude web distortion and web bend buckling.

The various ρ_{top} values were then achieved by adjusting the width and/or thickness of the top and bottom flanges. Flange width-to-thickness ratios were selected to satisfy slenderness and proportion limits established in AASHTO Section 6.10.2.2. Fig. 1 depicts a typical cross-section used in the FEA studies for $\rho_{top} \leq 0.5$. Note that sections with $\rho_{top} \geq 0.5$ are similar to its counterpart for $\rho_{top} \leq 0.5$, except that the top and bottom flanges are swapped.

3.3 Nonprismatic Sections

Nonprismatic sections, for which the cross-sectional properties of a beam are not uniform along an unbraced length, were studied extensively. The nature of the nonprismatic sections are described by the following parameters: (i) variations in flange thickness or width, (ii) location of the transition with respect to the brace points, and (iii) number of transitions along an unbraced beam segment.

For each nonprismatic case considered, the thickness and/or the width of the flanges were varied within the transition region (i.e. the region in which the flange dimensions change abruptly). Flange thicknesses were increased by the following multipliers: {1, 1.25, 1.5, 1.75, 2}. In a similar fashion, flange widths were increased by a different set of multipliers: {1, 1.15, 1.3, 1.5}. To simplify discussions, the increase in flange dimensions (thickness or width) is described as a multiplier to the weak-axis moment of inertia ($I_{y,top}$ or $I_{y,bot}$) of the base, smaller section.

Thus, a prismatic beam is represented by the case in which the $I_{y,top}$ multiplier = $I_{y,bot}$ multiplier = 1. I_y multipliers corresponding to an increased flange thickness included 1, 1.25, 1.5, 1.75, and 2, while I_y multipliers corresponding to an increased flange width included 1, 1.52, 2.20, and 3.375 (e.g. $1.5^3 = 3.375$). The largest flange transition considered in the study included an I_y multiplier of 6.75, in which the flange thickness was increased by 2 and the width by 1.5 ($2 * 1.5^3 = 6.75$).

For highly monosymmetric sections in the study for which $\rho_{top,base} \leq 0.2$, applying large I_y multipliers often resulted in flange dimensions that were deemed impractical for typical plate girder designs. As such, flange and cross-section proportion limits were imposed to filter out these special cases. Any nonprismatic beam with a resulting flange exceeding three inches in thickness or any unique cross-section for which $\rho_{top} < 0.091$ or $\rho_{top} > 0.91$ (i.e. to satisfy AASHTO Section 6.10.2.2) were filtered from the data presented herein. These limits ensure that the girders evaluated are efficiently designed and could be transported and lifted with conventional shipping and erection procedures during construction.

Note that a case in which the top flange multiplier exceeds the bottom flange multiplier was not considered, as this is uncommon for composite girder design. The $I_{y,top}$ multiplier was therefore either equal to or less than the $I_{y,bot}$ multiplier for all cases. By varying the bottom flange dimensions relative to the top flange dimensions, it is also apparent that the value of ρ_{top} is no longer constant along an unbraced length as is illustrated in Fig. 1.

Along with the flange widths and thicknesses, the location of the flange transitions was also varied in the parametric study. Increased flange sections are typically used in design at locations of maximum positive and negative moment, which are a function of the span configuration and boundary conditions. To cover the most common cases, three different flange transition schemes were considered in the study based on three span configurations found in bridge and building design: (i) simply-supported single spans, (ii) interior spans of continuous units, and (iii) end spans of continuous units. For the simple-span condition, flange transitions were taken as symmetric about the midspan of the beam; for the continuous span cases, transitions were considered in the negative moment regions at the ends of the beam. Note that the assumed span arrangement does not impact the boundary conditions in the finite element model; rather, it simply characterizes the flange transition scheme with which it is typically associated.

For each of these schemes, transitions at $0.1L$, $0.2L$, $0.3L$, and $0.4L$ of the full span (relative to the closest end of the beam) were evaluated. Cases in which the location of the top flange transition differed from the location of the bottom flange transition were also considered. For these special cases, the transitions occurred at some combination of $0.1L$, $0.2L$, $0.3L$, and $0.4L$ of the full span. The various flange transition schemes are depicted schematically in Fig. 2.

Lastly, this study investigated unbraced beam segments with multiple flange transitions. Cases with up to four total flange transitions along its unbraced length, resulting in a maximum of three unique cross-sections, were evaluated. Cases with numerous transitions are representative of long-span girders with no intermediate bracing. However, cases with fewer transitions are more common, especially as intermediate bracing is added during erection.

A specific case is depicted in Fig. 1 as an example. The figure illustrates the plate thicknesses used to develop the nonprismatic girder for the simple span case (S) with $I_{y,top}$ and $I_{y,bot}$ multipliers of 1 and 1.5, respectively. The two transitions for this specific example occur at $0.3L$ from each end, resulting in two unique cross-sections along the length: "small" (section A-A) and "large" (section B-B). The different combinations of these parameters are depicted schematically in Fig. 2. Figs. 1 and 2 are presented to provide the reader with the scale of the parametric study and not to highlight any specific geometry.

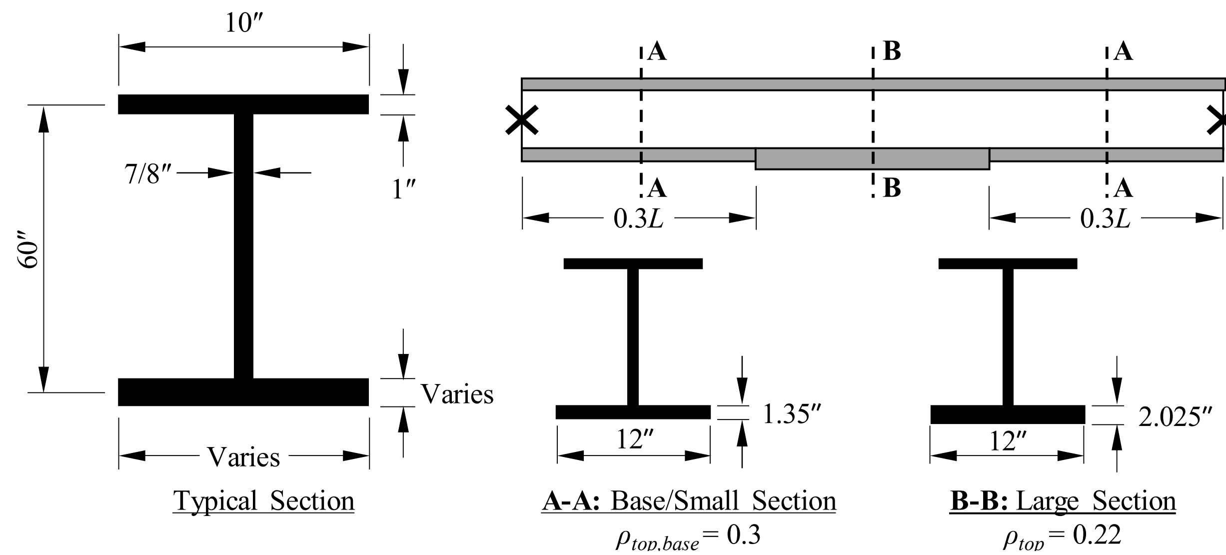

Figure 1: Typical cross-section used in the parametric study and an example showing how a simply-supported nonprismatic girder with flange transitions is developed

The flange transitions shown in Fig. 2 were also maintained for the different intermediate bracing schemes. To clarify, an example is presented in Fig. 3 for the simple span case, where the transitions occur at $0.3L$ from the beam ends (as noted earlier, transitions were also placed at 0.1L, 0.2L, and 0.4L from the ends). Fig. 3 shows the same beam with zero, one, and two intermediate braces. Note that for the two-brace case, the transition at $0.3L$ occurs beyond the limits of the unbraced segment considered; therefore, it is evaluated as a prismatic section for this specific case. A similar layout is considered for all transition locations and for all the continuous, interior span and continuous, end span cases.

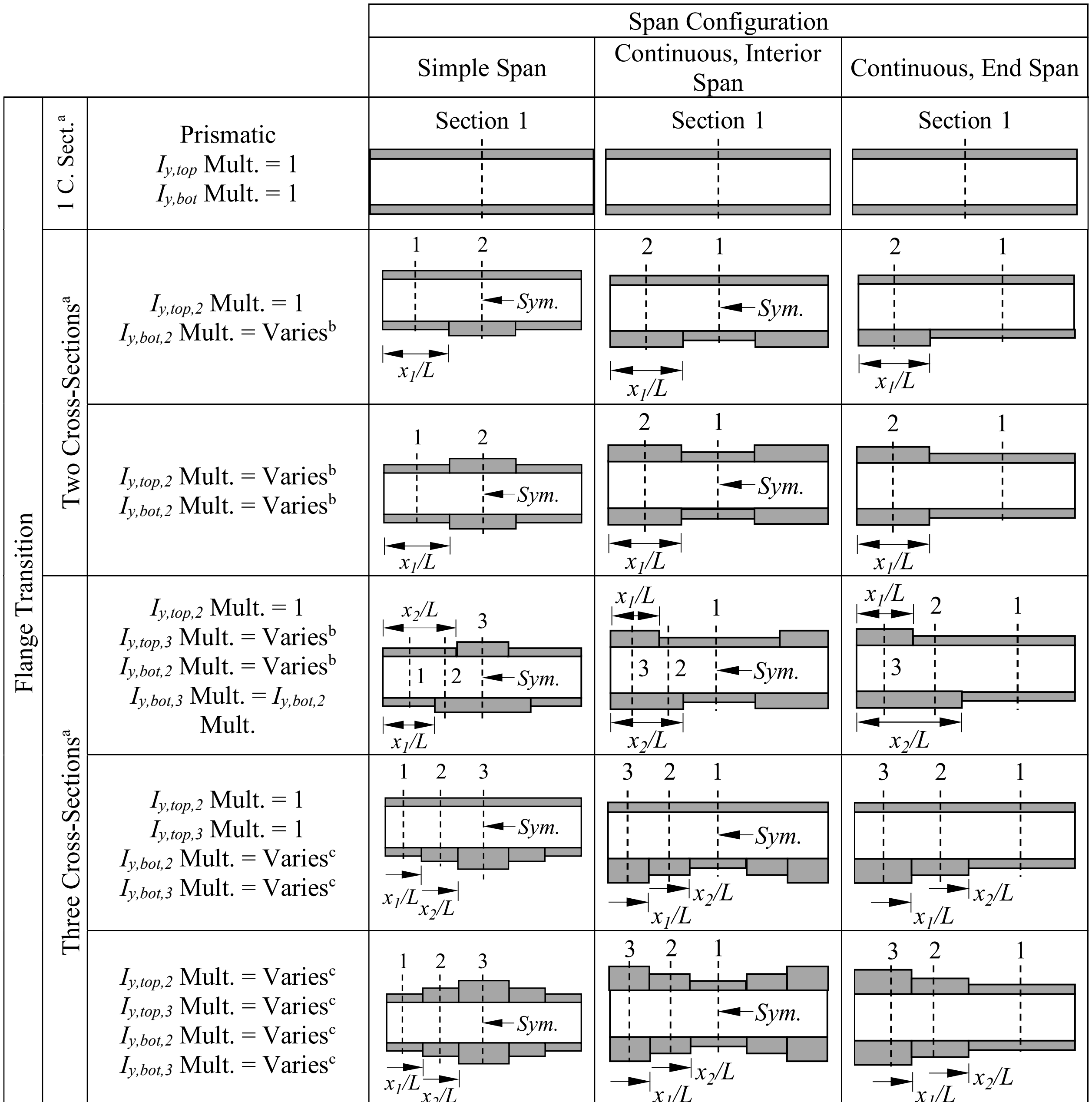

Note: Abbreviations: "Mult." = multiplier, "C. Sect." = cross-sections, and "Sym." = symmetric

[a] Represents the number of unique cross-sections along the unbraced length; x_i/L values vary and are either 0.1L, 0.2L, 0.3L, or 0.4L as previously outlined.

[b] For unbraced lengths with two cross-sections, "varies" indicates that the flange dimensions are increased within the transition region as previously outlined.

[c] For unbraced lengths with three cross-sections, "varies" indicates that the flange dimensions are increased at each new transition.

Figure 2: Flange transitions considered in the parametric study

Bracing Scheme		
Zero Intermediate Braces ($L_b = L$)	One Brace ($L_b = L/2$)	Two Braces ($L_b = L/3$)

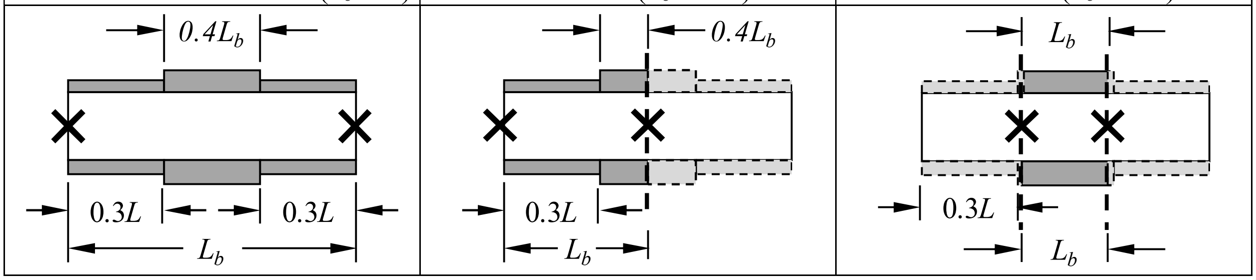

Figure 3: Flange transition cases for simply-supported condition with different intermediate bracing schemes

4. Finite Element Model and Interpretation of Results

The finite element software Abaqus (2017) was used to conduct the parametric studies. Elastic eigenvalue buckling analyses were performed to determine the critical buckling loads. Cross-sections of the girders including transverse stiffeners were modeled with shell elements. Transverse stiffeners were added at end supports and spaced at a distance equal to the girder web depth along the beam length to control local web buckling and distortion that may affect the LTB response. Simple supports conditions were considered, where vertical displacement was restrained at both beam ends and longitudinal displacement was restrained at only one end.

Brace points were represented by simple torsional support conditions, in which the top and bottom flange-to-web junctions were restrained against out-of-plane translation, but the cross sections were still free to warp. To remain consistent with most design specifications, the warping restraint contributions from adjacent, unbraced segments were conservatively neglected in the FEA models. Thus, the various intermediate bracing schemes were achieved in Abaqus by modeling only the unbraced segment of interest.

A mesh sensitivity analysis was performed before conducting the parametric studies to ensure the accuracy of the numerical model. A mesh size of 2 inches, which resulted in 30 elements along the web depth, was selected. An element aspect ratio as close to unity as practical was selected, which has been shown to work well in past studies (Wang 2013). By achieving good agreement between the FEA solutions and the exact theoretical solution for cases with prismatic sections, the assumed mesh density and boundary conditions were deemed suitable.

Uniform moment conditions were achieved by applying a force couple to the top and bottom flanges at each end of the unbraced segment. Rather than applying coupled point loads to the ends of the flanges, effective forces were distributed along the width of the respective flange and applied as a line load to preclude any localized buckling effects at the application of load. For example, if the effective flange force on a 10-inch wide flange is 1 kip, then a 0.10 kips/inch line load was applied along the edge of the flange width.

As introduced in the background section, there are two variables to consider when evaluating design specifications for LTB behavior under uniform-moment loading: (i) the theoretical buckling solution ($M_{cr,th}$) and (ii) the finite element solution for beam buckling under uniform moment ($M_{cr,FEA}$). For doubly- or singly-symmetric prismatic beams, FEA solutions for uniform-moment loading should be nearly identical to the theoretical solution in Eq. 1 (i.e. $M_{cr,th} \approx M_{cr,FEA}$). The results of this study corroborated this, as the FEA results were within ±2% of the theoretical solution.

Although Eq. 1 works well for estimating the LTB behavior of prismatic sections, the FEA results for nonprismatic beams under uniform moment will not generally agree with the results of Eq. 1 ($M_{cr,th} \neq M_{cr,FEA}$). The accuracy of the theoretical solution with respect to $M_{cr,FEA}$ is largely dependent on how the nonprismatic section properties are considered. As discussed previously, a length-weighted average approach for section properties is proposed. To evaluate the accuracy of proposed approach, the effective section factor (C_{eff}) is introduced. C_{eff} is defined as the ratio of the FEA solution under uniform moment ($M_{cr,FEA}$) to the LTB resistance computed from Eq. 1 ($M_{cr,th}$) as modified to account for nonprismatic section properties, and is given in the following expression:

$$C_{eff} = \frac{M_{cr,FEA}}{M_{cr,th}} \tag{4}$$

Values of C_{eff} less than unity indicate that the proposed method provides an unconservative estimate of the LTB resistance while values greater than unity indicate the opposite.

Various weighted-average approaches were investigated, but length-weighted averaging of the flange dimensions was ultimately found to produce the most consistent results for beams with stepped flange transitions. The length-weighted average method consists of computing an effective flange thickness and width (for both top and bottom flanges). The following expression applies to any generic section with zero or more unique transitions along the length of a flange (e.g. a nonprismatic flange with dimensions b_{small}, b_{medium}, and b_{large}):

$$b_{eff} = b_{small}[1 - (1 - x_{small})^n] + b_2(1 - x_{small})^n \tag{5}$$

where b_{eff} is the effective top or bottom flange width, b_{small} is the corresponding flange width of the small section, b_2 is the corresponding flange width of the second-smallest section, x_{small} is the fraction of the unbraced length consisting of the smallest section, and n is an exponent that transforms this weighted-average from a linear relationship ($n = 1$) to nonlinear relationship ($n > 1$). Eq. 5 essentially treats all sections larger than the smallest section (b_2, b_3,…, b_{large}) equivalent to the second-smallest section (b_2). For cases in which the top and bottom flange transitions occur at different locations along the unbraced length, Eq. 5 is to be applied independently for each flange with the appropriate x_{small} value for the flange under consideration.

The discussion above for Eq. 5 pertaining to the effective flange widths is also directly applicable for the computation of the effective flange thickness, t_{eff}. Once the effective flange dimensions are known, the pertinent section properties of this effective section can be computed for use in Eq. 1 or other similar expressions. Both linear and nonlinear relationships were investigated in this study (i.e. $n = 1$ and $n = 2$), and the results for each approach are presented herein.

Note that beams with variable-depth webs or more than three distinct cross-sections along the unbraced length have not been explicitly considered in this study. While the authors feel the methodology in Eq. 5 should still work well for cases with additional transitions and unique cross-sections, the majority of designs will likely have three or fewer unique cross-sections in a given unbraced length.

5. Results

For all combinations of variables in the parametric study, critical buckling loads with uniform-moment loading were determined using Abaqus and compared to the estimates provided by Eq. 1 using the length-weighted section properties. In total, 14,040 unique beam segments were analyzed. Figs. 4 and 5 show how Eq. 1 and the weighted-average section properties compare to the FEA results for various monosymmetric and/or nonprismatic sections. The figures provide only a sample of the full data set, but the results are representative of all cases considered.

In Fig. 4, the respective span-to-depth ratio and transition locations were held constant at L/h = 20 and 0.4L, while several extreme flange transition cases are presented. The following I_y multipliers, which are represented as {$I_{y,top}$ multiplier, $I_{y,bot}$ multiplier}, are considered: {1,1}, {1.75,1.75}, and {1,2.20}. In Fig. 5, the span-to-depth ratio and I_y multipliers are held constant at L/h = 20 and {1,1.75}, respectively, and the transition locations are varied. For both figures, a linear weighted-average approach for the effective section properties is employed (i.e. n = 1 in Eq. 5). Note that the degree of monosymmetry on the x-axis is taken with respect to $\rho_{top,base}$.

As noted earlier, a C_{eff} value of 1.0 indicates that the solution from Eq. 1 matches the FEA result exactly. Recall that for prismatic sections, the FEA solutions were generally found to be within 2% of Eq. 1. For this reason, subsequent discussions on the accuracy of the proposed methodology for nonprismatic sections are made relative to C_{eff} values of 0.98, not unity. It is deemed reasonable for nonprismatic members to have a similar level of uncertainty as for prismatic sections.

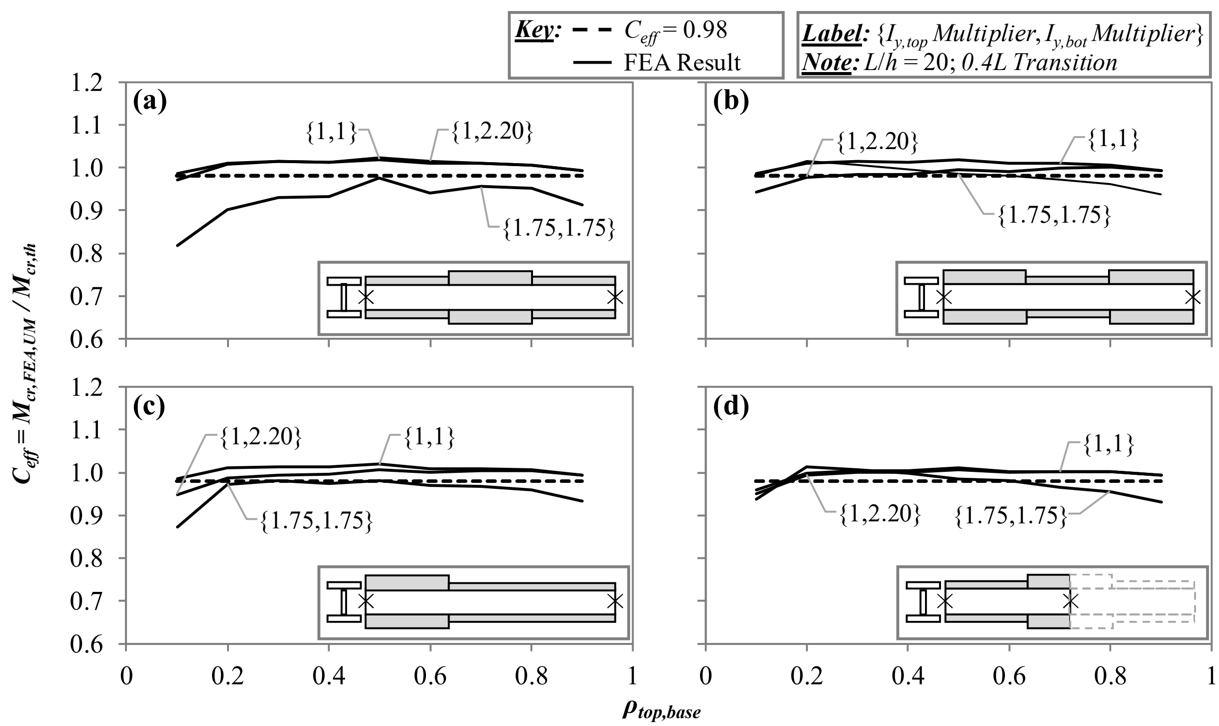

Figure 4: Evaluating the accuracy of Eq. 1 and weighted-average section properties (linear) for various degrees of monosymmetry, flange transitions, and intermediate bracing schemes

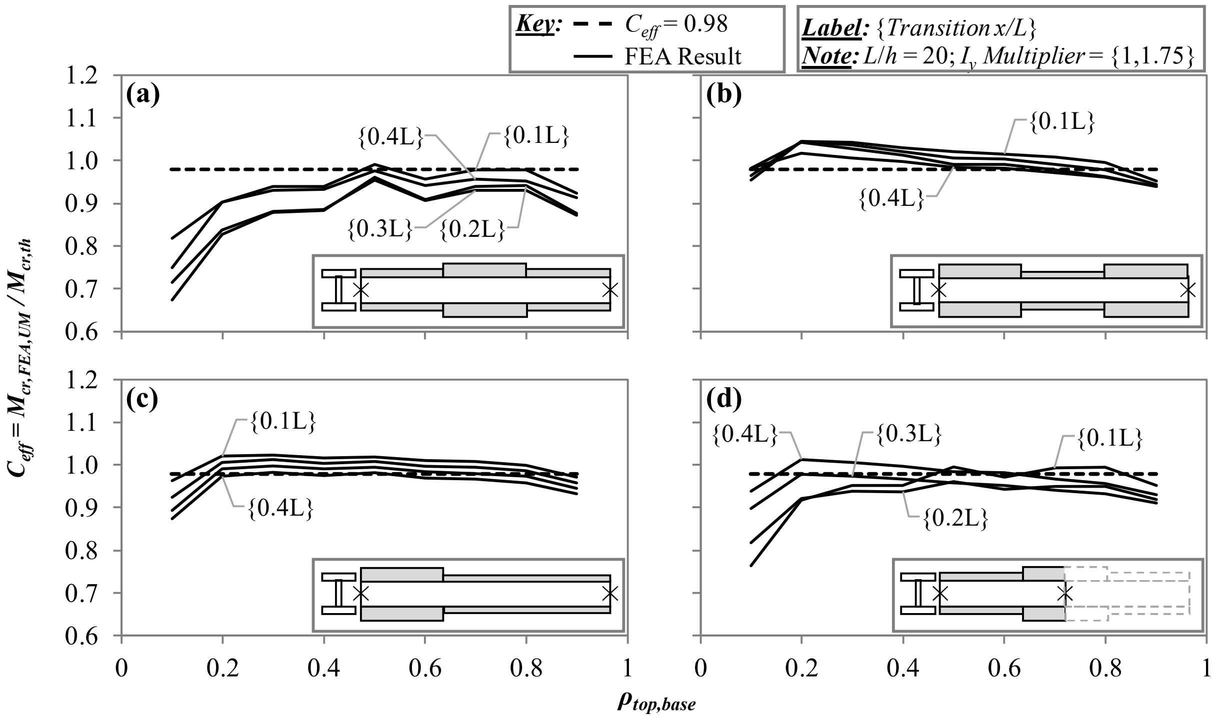

Figure 5: Evaluating the accuracy of Eq. 1 and weighted-average section properties (linear) for various degrees of monosymmetry, flange transitions, and intermediate bracing schemes

The following observations can be made from the results presented in Figs. 4 and 5:

- As expected, the C_{eff} results for prismatic beams (I_y multiplier of {1,1}) are generally within 2% of unity for all $\rho_{top,base}$ values.
- The accuracy of the linear weighted-average approach for section properties is dependent on the magnitude by which the flange dimension varies (I_y multiplier) and the location of the transition region.
- The linear weighted-average approach tends to overestimate the buckling capacity of the nonprismatic section ($C_{eff} < 0.98$) for highly nonprismatic sections with $0.2 \le \rho_{top,base} \le 0.5$, particularly for case *a* in Figs. 4 and 5.

Developing design guidelines to cover all flange transition schemes would be challenging, given the variability in the response. Instead, a unified approach to handling all nonprismatic sections is preferred. To safeguard against the unconservative results demonstrated in Figs. 4 and 5, a nonlinear form of Eq. 5 ($n = 2$) is proposed.

Fig. 6 demonstrates the benefits of implementing the nonlinear weighted-average approach over the linear approach for determining effective section properties of a nonprismatic beam. Here, the entire data set is presented, and the C_{eff} values are graphed as a function of ρ_{eff}, which is the degree of monosymmetry of the effective section. Additionally, only the most practical cases in which $0.2 \le \rho_{top,base} \le 0.5$ are shown. In total, nearly 6,500 prismatic and nonprismatic beams (of the over 14,000 evaluated) satisfied $0.2 \le \rho_{top,base} \le 0.5$ and are plotted in Fig. 6.

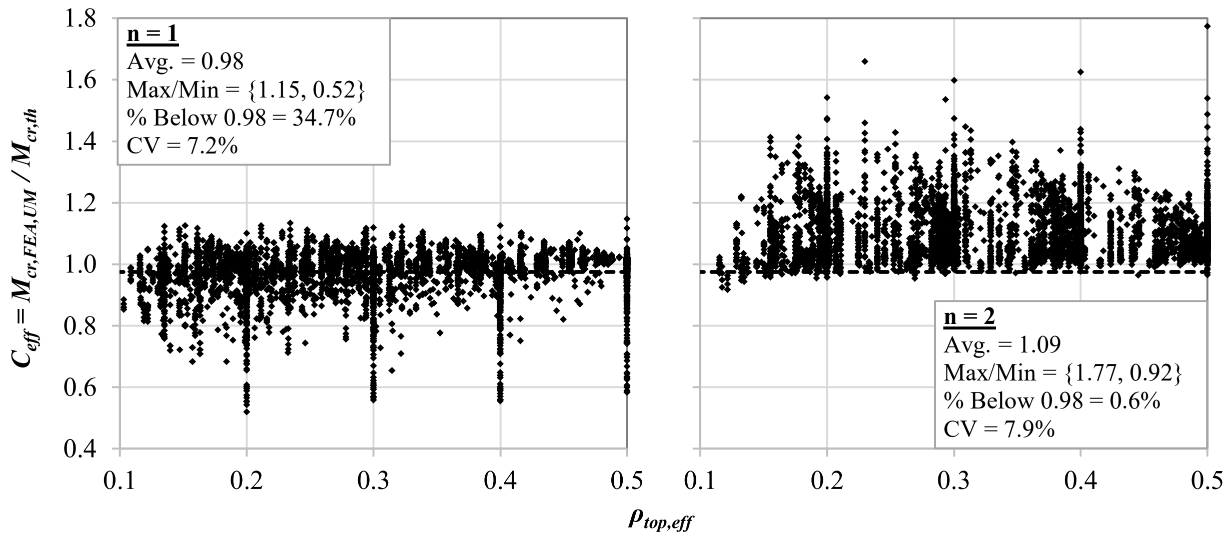

Figure 6: Evaluating the accuracy of linear (n = 1) and nonlinear (n = 2) weighted-average section properties for all nonprismatic beams in the parametric study

From Fig. 6, it is apparent that a value of $n = 2$ in Eq. 5 produce conservative and reasonable estimates of the effective section properties. The data points are largely shifted above the 0.98 benchmark value. With $n = 1$, Eq. 1 produces unconservative estimates of the buckling capacity for over 34% of the nonprismatic beams studied; in contrast, that number reduces to less than 1% with $n = 2$. The few unconservative cases correspond to highly monosymmetric beams with large I_y multipliers, which are less common in building and bridge applications. The few cases where C_{eff} exceeds 1.5 correspond to beams with three unique cross-sections where the majority of the nonprismatic beam segment consists of the "large" section.

On average, the nonlinear weighted-average approach produces a solution that is 9% conservative. As a reference, simply using the smallest section to characterize the entire unbraced segment (which is consistent with the current recommendations in AASHTO) results in nearly 20% conservatism on average and several cases in which C_{eff} exceeds 2.0, which many designers would likely deem overly conservative. Thus, it is evident that the proposed method is an improvement over the current methodology.

6. Summary and Conclusions

Current design specifications provide inadequate guidance on procedures to estimate the LTB resistance of nonprismatic beams, despite these conditions being relatively common in bridge and building applications. Past research on the topic has also been limited, and no studies have provided a simplified, general-use methodology for accurately predicting the LTB response. Acknowledging that design provisions must blend practicality and accuracy, the authors sought to develop proposed solutions that are simple to interpret and apply in design, while covering the most common conditions encountered in practice.

Based on the results presented in the preceding sections, it is concluded that using effective section properties based upon a nonlinear length-weighted average of the flange dimensions provides reasonable estimates for the LTB resistance of nonprismatic girders. For girder sections within practical values of ρ_{top}, these approximate solutions produce estimates on the order of 0-20%

conservative on average and are applicable for any unbraced beam segment with multiple flange transitions. Additionally, the results of this work can be easily implemented into the AISC and AASHTO specifications with minimal changes to the existing provisions and commentary.

Acknowledgements

The work documented in this paper was conducted in conjunction with an ongoing effort of a subcommittee of the AASHTO T14 (Steel Bridge Committee). The subcommittee has investigated improved solutions for singly-symmetric sections that may be either prismatic or nonprismatic along the unbraced length. The authors would also like to acknowledge Texas Advanced Computing Center (TACC) for providing the computing resources to conduct the extensive parametric studies.

References

Abaqus/CAE (2017). *Abaqus/CAE user's guide*.

AASHTO (American Association of State Highway and Transportation Officials). (2017). "LRFD bridge design specifications (8th ed.)." Washington, D.C.

AISC (American Institute of Steel Construction). (2016). "Specification for sructural steel buildings." Chicago, IL.

Galambos, T. V. (1968). *Structural members and frames*, Prentice Hall, Englewood Cliffs, NJ.

Gelera, K. M., and Park, J. S. (2012). "Elastic lateral torsional buckling strength of monosymmetric stepped i-beams." *KSCE Journal of Civil Engineering*, 16(5) 785-793.

Grubb, M. A., and Schmidt, R. E. (2012). *Steel bridge design handbook, design example 1: Three-span continuous straight composite steel i-girder bridge*, U.S. Department of Transportation, Federal Highway Administration, Washington, D.C.

Han, L., and Helwig, T. A. (2017). "Nonlinear behavior of global lateral buckling of i-girder systems." *Proc., Annual Stability Conference*, San Antonio, TX.

Helwig, T. A., Frank, K. H., and Yura, J. A. (1997). "Lateral-torsional buckling of singly symmetric i-beams." *J. Struct. Eng.*, 123(9) 1172-1179.

Reichenbach, M. C., Liu, Y., Helwig, T.A., and Engelhardt, M. D. (2019). "Moment gradient factors for singly-symmetric I-sections." *Proc., Annual Stability Conference*, St. Louis, MO.

Park, J. S., and Stallings, J. M. (2003). "Lateral-torsional buckling of stepped beams *J. Struct. Eng.*, 129(11) 1457-1465.

Slein, R., and White, D. W. (2019). "Streamlined design of nonprismatic i-section members." *Proc., Annual Stability Conference.* St. Louis, MO.

Timoshenko, S. P., and Gere, J. M. (1961). *Theory of elastic stability*, McGraw-Hill. New York, NY.

Trahair, N. S. (1993). *Flexural-torsional buckling of structures*, CRC. Boca Raton, FL.

Wang, W. (2013). *A Study of Stiffness of Steel Bridge Cross Frames*, PhD Dissertation, University of Texas at Austin, Austin, TX.

Ziemian, R. D. (2010). *Stability design criteria for metal structures: Sixth edition*, John Wiley & Sons, Inc. Hoboken, NJ.